Preliminary Results at the Ultra Deep X-ray Lithography Beamline at CAMD

Georg Aigeldinger *,**; Phil Coane***; Ben Craft*; Jost Goettert*; Sam Ledger***; Zhong Geng Ling*; Harish Manohara* and Louis Rupp*

* Center for Advanced Microstructures and Devices (CAMD), Louisiana State Univ., 6980 Jefferson Hwy., Baton Rouge, LA 70806 (gaigeld@unix1.sncc.lsu.edu)
** Institute for Microsystem Technologies, Univ. Freiburg, Germany
***Institute for Micromanufacturing, Louisiana Tech Univ., PO Box 10137, Ruston, LA 71272 (pcoane@coes.latech.edu)

ABSTRACT

The Center for Advanced Microstructures and Devices (CAMD) at Louisiana State University supports one of the strongest programs in synchrotron radiation microfabrication in the USA and, in particular, in deep X-ray lithography (DXRL). Synchrotron radiation emitted from CAMD’s bending magnets has photon energies in the range extending from the infrared to approximately 20 keV. CAMD operates at 1.3 and 1.5 GeV, providing characteristic energies of 1.66 and 2.55 keV, respectively.
CAMD bending magnets provide a relatively soft X-ray spectrum that limits the maximal structure height achievable within a reasonable exposure time to approximately 500 µm. In order to extend the X-ray spectrum to higher photon energies, a 5 pole 7T superconducting wiggler was inserted in one of the straight sections. A beamline and exposure station designed for ultra deep X-ray lithography (UDXRL) was constructed and connected to the wiggler. First exposures into 1 mm and 2 mm thick PMMA resist using a graphite mask with 40µm thick gold absorber has been completed.

Keywords: Ultra Deep, X-Ray Lithography, Wiggler, X-ray Mask, LIGA.

INRODUCTION

The Louisiana State University, CAMD facility is a University owned and operated Synchrotron Light Source built for the microfabrication and analytical sciences. The center supports one of the strongest programs in synchrotron radiation microfabrication in the USA and, in particular, in deep X-ray lithography (DXRL) for high aspect ratio microstructure fabrication. DXRL is the key step for the LIGA process.[1] LIGA is a German acronym, which describes the lithography, electroforming (galvanoformung), and molding (abformung) steps used to create high-aspect ratio microstructures. DXRL enables the patterning of tall microstructures with heights ranging from 100 µm to 1000 µm and aspect ratios of 10 to 50. DXRL provides lithographic precision of placement, smallest feature sizes in the micrometer range and sub-micrometer details over the entire height of the structures. [1]

CAMD participated successfully in the HI-MEMS Alliance that has established an infrastructure and network to support prototyping and distributed manufacturing based on DXRL. The HI-MEMS Alliance has provided a multi-user LIGA service (LIGA-MUMPS) to users from academia and industry.[2] CAMD functions as the “Print Shop” for the Alliance, providing routine operation for the exposure of thick resists up to 300 µm. CAMD was awarded “Center of Excellence” for its activities within the Alliance in 1997.

CAMD operates at 1.3 and 1.5 GeV electron energies. The characteristic energy of the spectrum from a bending magnet (radius of curvature = 2.928m) is 1.66 keV and 2.55 keV, respectively. Currently three beamlines, dedicated to X-ray lithography and DXRL are operational. Two are operated by CAMD using

Part of the Symposium on *Design, Test, Integration, and Packaging of MEMS/MOEMS,* Bernard Courtois, Selden B. Crary, Kaigham J. Gabriel, Jean Michel Karam, Karen Markus, Andrew A. O. Tay, Editors, Proceedings of SPIE Vol. 4019 (2000)

in-house designed scanners; the Institute for Micromanufacturing (IfM), Louisiana Tech University [3] operates the third, using a commercial stepper from Jenoptik. [4]
A 200 m^2 clean room with a variety of processing, metrology and characterization equipment (e.g. optical pattern generator, thin metal film deposition, UV exposure station, reactive ion etching and ion milling, electroplating station and optical, electron and atomic force microscopes) allows pre- and post- processing capability at CAMD and is also available to external users.

CAMD provides a relatively soft X-ray spectrum that limits the maximal structure height achievable within a reasonable exposure time to approximately 500 μm. In order to extend the X-ray spectrum to higher photon energies without disturbing the ring structure and the conditions of the already installed beamlines, a 5 pole 7T superconducting wiggler was inserted in one of the straight sections. [5,6] With a 7T magnetic field the wiggler defines a radius of curvature of ca. 0.7 m. The corresponding power spectrum is shown in Fig. 1 together with the spectra of the bending magnets at 1.3 and 1.5 GeV. The spectra are also compared to that of the UDXRL beamline (X27B) at Brookhaven National Lab (NSLS).
A significant power output of photons with energies up to 40 keV is achieved at the CAMD wiggler and it shows approximately the same total power for similar conditions like at NSLS X27B with a slightly harder spectrum. Prior to the availability of the wiggler beamline preliminary UDXRL exposures have been conducted at the NSLS X27B beamline. [7] The new wiggler source provides CAMD with a powerful tool to effectively expose tall microstructures up to several millimeters. The higher integral power also offers the potential to improve the sample throughput by reducing exposure times.

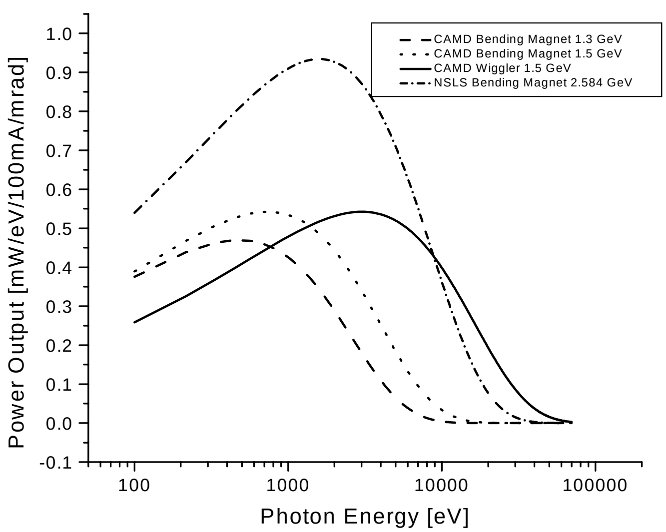

CAMD
Bending Magnet at 1.3 GeV:
E_c = 1.66 keV, P_{tot} = 1.37 W/mrad/100mA

Bending Magnet at 1.5 GeV:
E_c = 2.55 keV, P_{tot} = 2.44 W/mrad/100mA

Wiggler Magnet at 1.5 GeV, 7T:
E_c = 10.5 keV, P_{tot} = 9.92 W/mrad/100mA

NSLS
Bending Magnet at 2.584 GeV:
E_c = 5.57 keV, P_{tot} = 9.1 W/mrad/100mA

Fig. 1: Spectral power output from CAMD lithography beamlines for 100 mA electron current compared to NSLS X27B DXRL beamline.

WIGGLER BEAMLINE AND EXPOSURE STATION

The setup of the beamline and exposure station constructed and built at CAMD is shown in Fig. 2 in a side view. The wiggler radiation is passing through the UHV beamline from left to right in Fig. 2. The radiation is leaving the storage ring through a special dipole chamber (not shown in picture). After passing through a manual gate valve, a water-cooled copper aperture is defining a maximum horizontal acceptance angle of 9 mrad. A photon and a Bremsstrahlungsshutter ensure a safe operation of the beamline. The radiation is extracted from inside the storage ring via a shield wall through tube (25 mm high x 100 mm wide) that is covered with additional lead bricks for radiation protection. After passing the final gate valve 3 and a beamline terminating Be window, 250 μm thick, 120 mm x 15 mm open aperture, the radiation is exiting into atmosphere. The Be-window is built to common standards [8] and can withstand a radiation power of more than 10 W/cm vertically integrated. The Be foil of the window is vacuum brazed to a copper block

that is cooled to 20°C. The Be-window terminates the UHV section of the beamline at about 10 m distance of the source point.
The atmospheric side of the Be window is surrounded by a helium flood enclosure to protect the sensitive beryllium from moisture and from ozone produced by radiation interacting with the atmosphere. The radiation is then extracted from the He-chamber through a 100 µm thick Kapton window. The radiation is traveling through a 30 cm wide air gap before it hits the X-ray mask. The air gap allows both easy optional filter placement to adapt top to bottom dose ratios to resist thickness and setting a defined aperture to minimize the heat load on the mask.
The wiggler beam can be monitored using a diagnostic flag installed in the 6 ways cross in the front of the beamline. In the 10-inch cross, two filters (1 mm and 2 mm thick Al) are mounted in front of a phosphoresced Cu plate acting as a fluorescent screen. The screen can be monitored via a glass view port using a CCD camera with magnifying optics. The 1 mm Al filter blocks out practically all radiation below 10 keV energy, the 2 mm Al filter all below 15 keV. Furthermore, an 80% transparent Ta mesh is mounted below the screen and can be used as an *in-situ* photon monitor to better control the actual incident photon flux.

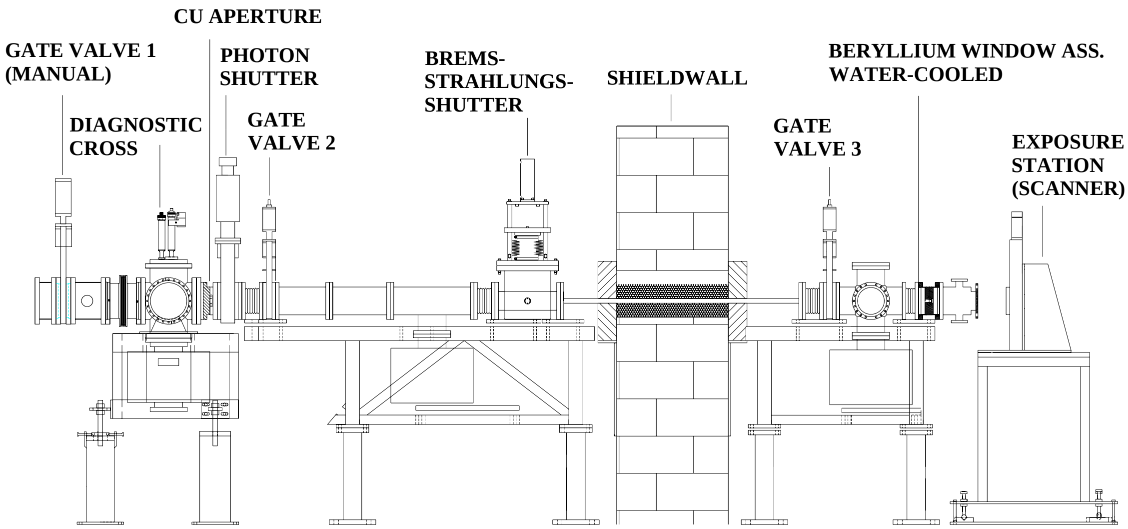

Fig. 2: Layout of the CAMD wiggler beamline (side view).

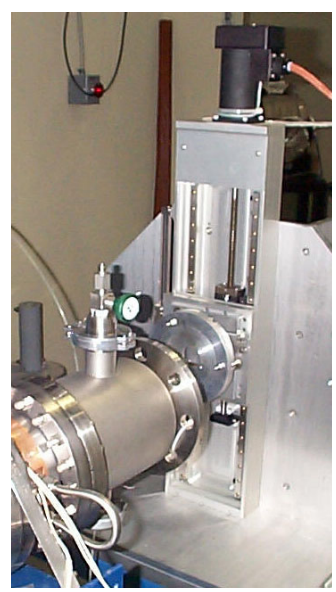

Fig. 3:
Scanner setup and He enclosure mounted at the end of the wiggler beamline.

The beamline is terminated with an in-air exposure station (Fig. 3). It consists of a vertical scanning stage designed with a sled driven by a stepping motor and spindle mounted to an optical table placed on a kinematic mount for precise adjustment on the floor. Currently, the maximum scan speed is 10 cm/s and the vertical scan length can be set to a maximum of 30 cm. This scan length allows for long scans and multi sample exposures when samples are mounted lined up vertically. The scanner is controlled by a personal computer with a basic user interface. For compatibility reasons the wafer-mask assembly is similar to the fixtures of the other CAMD beamline exposure station. In the future additional water-cooling of the mask/substrate assembly is foreseen to minimize the thermal load on the assembly during the exposure.

GRAPHITE MASKS

For X-ray based micromachining, mask fabrication for deep or ultra-deep X-ray lithography (DXRL and UDXRL, respectively) is a critical requirement as it determines costs as well as turn-around time. However, until now no standard mask technology has been developed that is accepted by all users. For example, in DXRL microstructures of up to 1 mm are produced using high-energy photons over a range from 5 keV to 15 keV. Here, a typical X-ray mask consists of fragile 2 µm thick silicon or titanium membrane and a gold absorber thickness varying from 5 µm to 15 µm [9,10]. For the fabrication of taller microstructures in UDXRL, photons with energies up to 40 keV are used. In this case, relatively thick beryllium (300-600 µm) [11], silicon substrates (50-400 µm) [12], and graphite substrates (125-250 µm) [13] are suitable. The required contrast is assured by using a gold absorber with thickness up to 50 µm. A compromise, offering reduced costs and safe handling on one hand and the potential for standardization for DXRL and UDXRL applications on the other hand, is using rigid graphite as the mask membrane [13,14].

For these experiments, off-the-shelf rigid graphite 4“ wafers 125 µm thick and of 99.95% purity were used [15]. The mask pattern was generated from a Ti mask used as an intermediate mask. The Ti mask pattern was transferred into a 10 µm thick spin-coated PMMA resist using soft x-rays. After development of the irradiated resist, electroplating of the Au absorber pattern up to 5 µm followed. Prior to electroplating, the backside was covered with an optical resist to prevent plating. The 5 µm thick Au pattern was used as an intermediate mask. Before stripping the resist a thick PMMA sheet (up to 100 µm) was solvent bonded onto the backside of the wafer. X-ray lithography was repeated to transfer the intermediate mask pattern into the thick PMMA resist using the same graphite sheet. The exposed areas were then dissolved in the GG developer at room temperature and the working mask was plated with Au absorbers approx. 40 µm high. Stripping the PMMA resist and etching off the intermediate mask using aqua regia achieved the final mask. The process sequence is described in more detail in [14].

Fig. 4a shows as an SEM picture of the working mask pattern of a gear train made in ~40 µm Au. On the close-up view in Fig. 4b an approx. 5 µm high lip at the edges of the absorber pattern occurs resulting from the plating conditions. However this should not compromise the patterning capability of the mask Also at the interface to the graphite surface some underplating can be seen indicating that the PMMA resist did not adhere perfectly at this point.

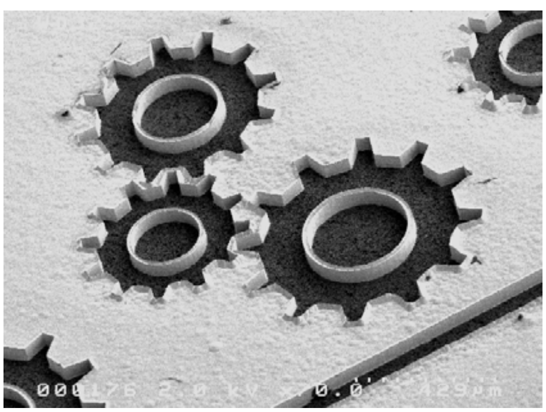

Fig. 4a: SEM picture of a Au absorber pattern of a gear train on a graphite sheet.

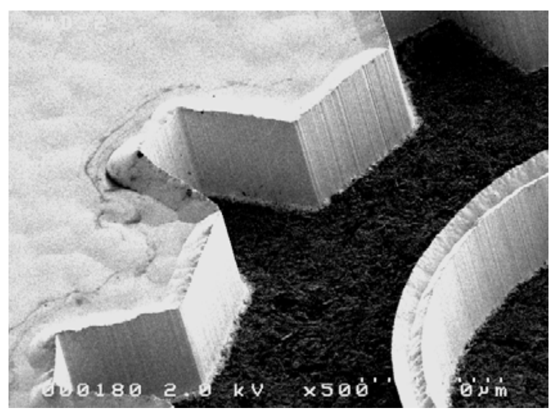

Fig. 4b: Close-up view of the the tooth pattern of a gear.

Furthermore, vertical striations can be seen on the sidewall of the tooth that is known for X-ray masks on graphite. [14] These striations do not exist on the Ti mask and may be caused by in-homogeneities in the graphite sheet. The consequences are rougher sidewalls of the PMMA microstructure.

Part of the Symposium on *Design, Test, Integration, and Packaging of MEMS/MOEMS,* Bernard Courtois, Selden B. Crary, Kaigham J. Gabriel, Jean Michel Karam, Karen Markus, Andrew A. O. Tay, Editors, Proceedings of SPIE Vol. 4019 (2000)

EXPOSURE TESTS

First exposures at the Wiggler beamline were performed in September 1999. The exposure tests where conducted with the graphite mask previously described. PMMA resist of different thickness were solvent bonded onto Si wafers used as substrate. Most of the Si substrates have been coated with a 0.5 μm thick Cu layer. Some substrates were prepared with a Cu/Ti metal layer as has been developed within the Hi-MEMS Alliance. [2] The proximity gap was 1 mm and the scan length 60 mm. Scan speed was 10 cm/s. For these exposures the wiggler was set at a 6T center magnetic field and the storage ring was operated at electron energy of 1.5 GeV. The characteristic energy of the photon spectrum was 6.2 keV. The average ring current was 50 mA during the exposures.

For these parameters the exposure time for a 1 mm thick PMMA resist was approx. 2 hours with a bottom dose of 4 kJ/cm^3 and a top to bottom ratio of 2.3. After exposure there appeared no foaming on the resist surface. Development of the sample was done in GG developer for 36h at 20º C in a beaker with magnetic stir. Figs. 5a - c show SEM pictures of microstructures on this sample. In Fig. 5a the accurate pattern transfer even of the 10 μm wide PMMA ring can be seen. In the close up view of the tooth pattern in Fig. 5b there is hardly any rounding of the top of the structure identifiable indicating that the underplated Au did not effect the pattern transfer accuracy and that fluorescent effects stemming from the graphite sheet can be neglected [14]. Furthermore the striations shown on Fig 4b on the mask are also precisely replicated in the PMMA structure. This results in an increased sidewall roughness of ~150-200 nm Ra value. [14]

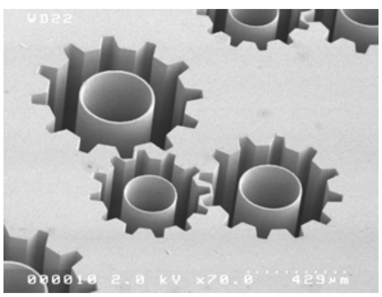

Fig. 5a: SEM picture of a gear train assembly exposed into 1 mm thick PMMA resist at the wiggler beamline.

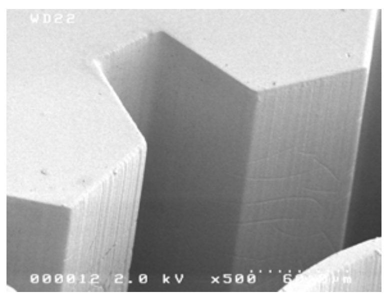

Fig. 5b: Close-up view of the tooth sidewall.

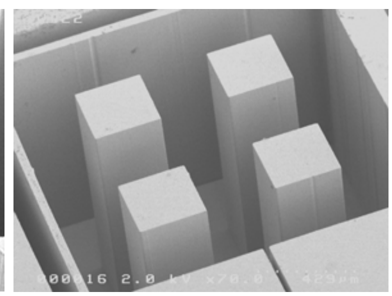

Fig 5c: Array of posts proving that the resist has been completely removed in the exposed areas.

Also from this SEM picture very fine horizontal cracks appear on the sidewall indicating that both a certain dose deposition above the threshold dose for PMMA as well as the extremely long development time had some impact on the PMMA structure. An array of posts 300 μm wide shown in Fig. 5c is documenting that at least in wider areas the exposed resist has been fully developed to the substrate.

For comparison this mask has also been used for exposure tests at a bending magnet beamline operated at 1.3 GeV. In this case the resist was only 300 μm thick in order to achieve reasonable exposure times. The structures shown in Figs. 6a and 6b are directly comparable to the pattern shown in Figs. 5a and 5b. Although the effective exposure spectra taking into account the vacuum window, mask and filter absorption are extremely different as can be seen from Fig. 7 there is hardly any difference in the exposure results demonstrated by the SEM pictures. This proves the good contrast of the graphite mask and its application for both DXRL and UDXRL. However, there is a difference in crack formation on the sidewalls that is most likely caused by the longer development time of the wiggler sample.

The wiggler spectrum is filtered by 250 μm Be window, 100μm Kapton, 125 μm graphite mask and 30 cm of air. The maximum is at 10 keV and the total incident power is 4.5 W/mrad at 100 mA. The bending spectrum is filtered by 200 μm Be and 125 μm graphite mask, only, resulting in a maximum of 5 keV and a total incident power of 0.15 W/mrad. taking into account all filter absorption. Compared to the exposure results achieved with a graphite mask sidewalls from the Ti mask are much smoother as can be seen in Figs. 8a and 8b. In this case a 200 μm thick PMMA sample has been exposed. There are no measurable striations and the sidewalls are perfectly smooth.

Part of the Symposium on *Design, Test, Integration, and Packaging of MEMS/MOEMS,* Bernard Courtois, Selden B. Crary, Kaigham J. Gabriel, Jean Michel Karam, Karen Markus, Andrew A. O. Tay, Editors, Proceedings of SPIE Vol. 4019 (2000)

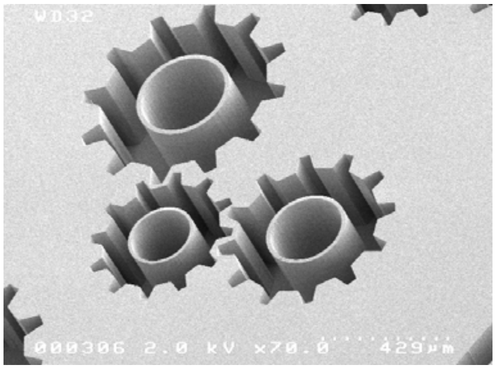

Fig. 6a: SEM picture of a gear train assembly exposed into 300 μm thick PMMA resist at the bending magnet beamline at 1.3 GeV.

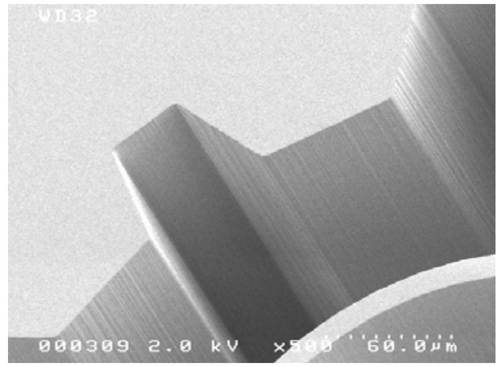

Fig. 6b: Close-up view of the tooth sidewall.

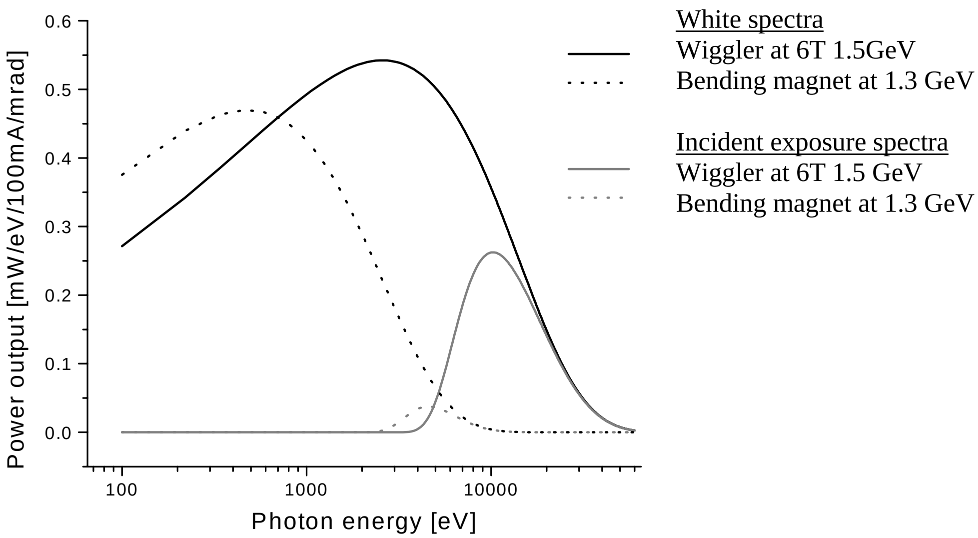

Fig. 7: Comparison of power spectra used for exposures at the wiggler and a bending magnet beamline.

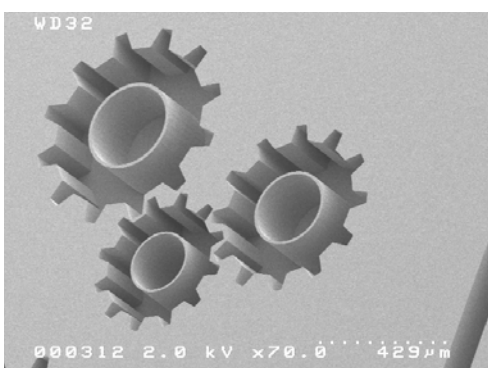

Fig. 8a: SEM picture of a gear train assembly exposed into 200 μm thick PMMA resist at the bending magnet beamline at 1.3 GeV using a Ti mask.

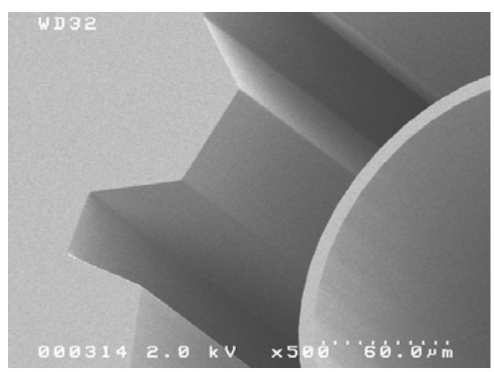

Fig. 8b: Close-up view of the tooth sidewall.

Part of the Symposium on *Design, Test, Integration, and Packaging of MEMS/MOEMS,* Bernard Courtois, Selden B. Crary, Kaigham J. Gabriel, Jean Michel Karam, Karen Markus, Andrew A. O. Tay, Editors, Proceedings of SPIE Vol. 4019 (2000)

CONCLUSIONS

With the installation of the wiggler beamline CAMD has improved and strengthen its X-ray lithography based mcirofabrication program towards Ultra deep X-ray lithography. Exposure conditions at the wiggler beamline are compatible to similar hard X-ray beamlines at other synchrotron sources and will allow the fabrication of tall, several millimeter high microstructures in a reasonable time. The set-up will also enable multi-substrate and/or large area substrates exposures optimizing the sample throughput.
Graphite membranes provide a suitable mask technology for both DXRL and UDXRL exposures. However, the current status of this mask technology still needs further improvement to achieve comparable results with thin membrane masks. Although the first exposure results in 1 mm tall microstructures are encouraging further optimization of the process parameters and exposure conditions are needed to fabricate defect-free high-aspect ratio microstructures.

ACKNOWLEDGEMENTS

The authors would like to thank the CAMD accelerator group for their technical support and after-hour operation of the machine. Special thanks to Kun Lian (CAMD) for electroplating the graphite mask used in this experiments and Robert Giasolli (IfM) for substrate preparation and sample inspection. Yohannes Desta (LSU μSET group) provided the Titanium mask that was used for this work. Work completed at CAMD was supported in part by the U S. Defense Advanced Research Projects Agency under contract number BAA N66001-97-6902.

REFERENCES

1. C. Friedrich et al: “High Aspect Ratio Processing” in: P. Rai-Choudhury (Ed.) Handbook of Microlithography, Micromachining and Microfabrication,Vol.2 (1997), pp. 299-377.
2. http://www.memsrus.com/cronos/svcsliga.html
3. http://www.latech.edu/tech/engr/ifm/
4. http://www.jo-mikrotechnik.com/
5. V. Saile et al: “Deep X-ray Lithography with a tunable wavelength shifter at CAMD”, J. of Synchrotron Rad., 1998, 5 1095-1098.
6. Manohara, H: “Development of Hard X-ray Exposure Tool for Micromachining at CAMD.” Proc. Of the 15. Int. Conference on Applicaitoin of Accelerators in Research and Industry: II, pp. 618-621, Nov. 1998.
7. G. Aigeldinger et al: “Simulating 3-Dimensional Deep X-ray Lithography Using the CXrL Toolset”, Tech. Proc. of MSM 1998, pp. 374-379.
8. http://dxchange.aps1.anl.gov:3000/
9. C. Khan Malek, R. Wood, B. Dudley, Z. Ling, V. Saile; SPIE Proc. on Microlithography and Metrology in Micromachining II, Vol. 2880, (1996), pp. 160-170.
10. W.K. Schomburg, H.J. Baring, P. Bley; Microelectronic Engineering 13, (1991), pp. 323-326.
11. F.J. Pantenburg, S. Achenbach, M. Sesterhenn; FZKA report 6080, Forschungszentrum Karlsruhe (1998), pp. 77-82.
12. J. Klein, H. Guckel, D.P. Siddons, E.D. Johnson; Microsystem Technologies 4 (1998) 70-73.
13. P. Coane et al: “Fabrication of HARM Stuctures by Deep-X-ray Lithography Using Graphite Mask Technology. Proc. HARMST ’99 Book of Abstracts, pp. 92-93 Kisarazu, Japan (1999).
14. P. Coane et al: “A Graphite-based X-ray Mask for Deep and Ultra-deep X-ray Lithography, J. Vac. Sci.Technol, B166(6) (Nov/Dec 1998), pp. 3618-3624.
15. Goodfellow Cambridge Limited, Cambridge, England, catalog 1995/96.